


# Decarbonization potential of floating solar photovoltaics on lakes worldwide

Received: 22 March 2023

Accepted: 7 May 2024

Published online: 4 June 2024

 Check for updates

R. Iestyn Woolway<sup>1</sup>✉, Gang Zhao<sup>2</sup>, Sofia Midauar Gondim Rocha<sup>3</sup>,  
Stephen J. Thackeray<sup>4</sup> & Alona Armstrong<sup>3,5</sup>

As climate change progresses, there is increasing emphasis on net zero and energy system decarbonization. Several technologies are contributing to this agenda, but among these, the growth of solar photovoltaics has consistently exceeded all projections. With increasing land-use pressures, and the expense of building-mounted photovoltaics, water surfaces are increasingly being exploited to host these technologies. However, to date, we lack an understanding of the global potential of floating solar photovoltaics and, as such, we do not yet have sufficient insight to inform decisions on (in)appropriate areas for future deployment. Here we quantify the energy generation potential of floating solar photovoltaics on over 1 million water bodies worldwide (14,906 TWh). Our analysis suggests that with a conservative 10% surface area coverage, floating solar photovoltaics could produce sufficient energy to contribute a considerable fraction (16%, on average) of the electricity demand of some countries, thus playing an important role in decarbonizing national economies.

Decarbonization of the global economy has become increasingly urgent as anthropogenic climate change progresses. Low carbon energy generation is fundamental to this decarbonization, and within this sphere, the growth of solar photovoltaics (PVs) has consistently exceeded all projections. Indeed, solar energy is predicted to be the dominant renewable energy source by 2050<sup>1</sup>. This rapid growth is attributed to cost effectiveness, the global nature of the resource and flexibility in deployment. Deployment flexibility has enabled the installation of ground- or building-, and more recently, water-mounted or floating systems<sup>2</sup>. Floating solar photovoltaics (FPVs), known colloquially as ‘floatovoltaics’, typically consist of an array of PV modules mounted upon a series of floats, moored into position on the surface of a water body. A growing body of evidence suggests that FPVs have several advantages over conventionally deployed PVs. For example, FPVs avert the need for land-use change where the alternative is a ground-mounted system; this is particularly beneficial in land-scarce countries and regions with high land prices<sup>3</sup>. Moreover, FPVs have also been shown to reduce evaporative losses, potentially providing

vital water savings for drought-stricken areas<sup>4</sup>. Finally, FPV systems have lower temperatures, and thus higher efficiencies, compared with land-based systems<sup>5,6</sup>. These advantages have driven rapid deployment of FPVs around the world in recent years, particularly on artificial water bodies<sup>7,8</sup>. This growth is anticipated to continue, capitalizing on the estimated 5 million km<sup>2</sup> of Earth’s surface area that is covered by lakes and reservoirs<sup>9</sup>. Such expansion could provide the potential for FPVs to meet a considerable proportion of current and future energy demands at local to regional scales<sup>7</sup>. However, to date, we lack an understanding of global FPV potential that moves beyond considerations of theoretical maximum capacity to take into account the impact of global variation in several important determining factors such as water body size and suitability, solar energy receipts, climatic conditions and energy demand. As such, we do not yet have sufficient insight to inform decisions on (in)appropriate areas for future deployment.

In this study, we quantify the energy generation potential of FPVs on over 1 million water bodies (>0.1 km<sup>2</sup> in surface area) worldwide, including both natural and artificial lakes and reservoirs

<sup>1</sup>School of Ocean Sciences, Bangor University, Anglesey, Wales, UK. <sup>2</sup>Key Laboratory of Water Cycle and Related Land Surface Processes, Institute of Geographic Sciences and Natural Resources Research, Chinese Academy of Sciences, Beijing, China. <sup>3</sup>Lancaster Environment Centre, Lancaster University, Lancaster, UK. <sup>4</sup>Lake Ecosystems Group, UK Centre for Ecology & Hydrology, Lancaster, UK. <sup>5</sup>Energy Lancaster, Lancaster University, Lancaster, UK. ✉e-mail: [iestyn.woolway@bangor.ac.uk](mailto:iestyn.woolway@bangor.ac.uk)

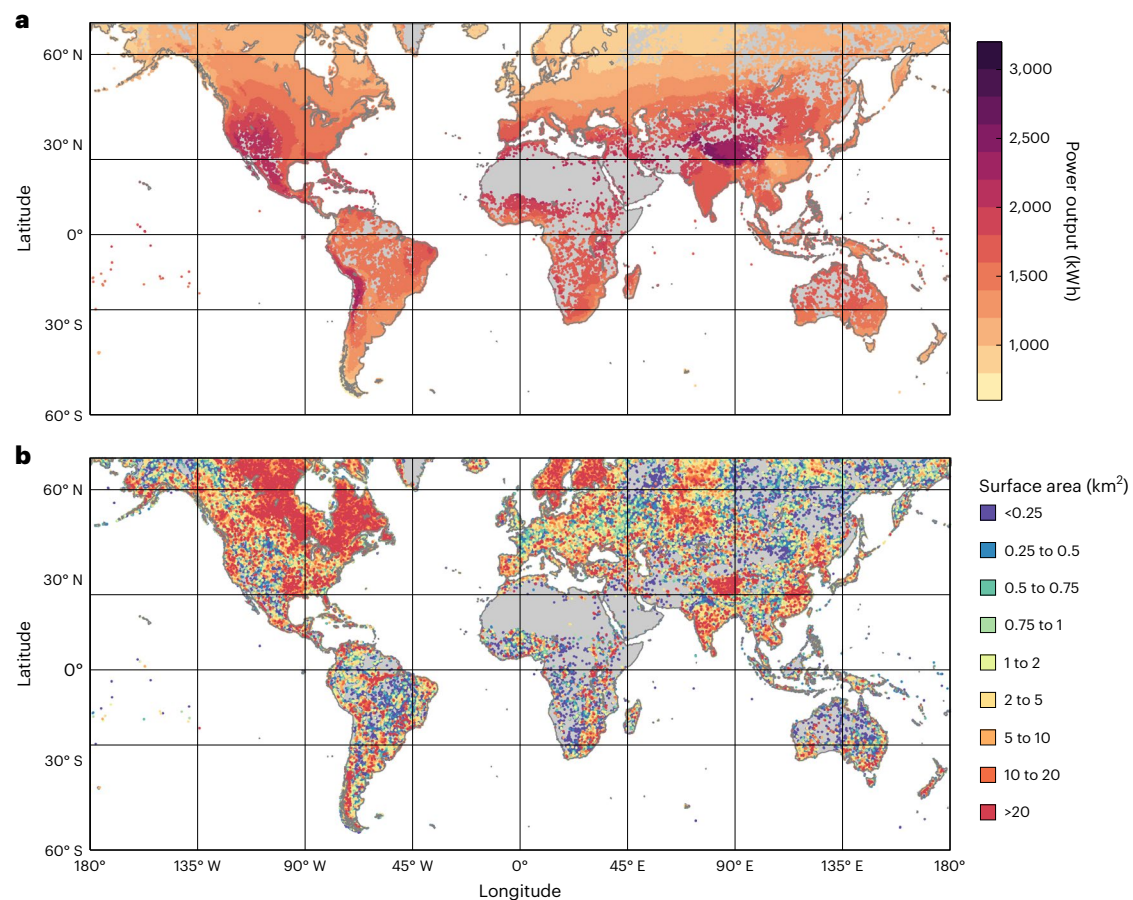


**Fig. 1 | Global variations in theoretical FPV power outputs and water body surface area. a, b.** Shown, for each of the >1 million water bodies considered in this study, are the calculated annual power output of a 1 kW FPV system, calculated from GSEE (Methods) (a) and the median surface area (km<sup>2</sup>) (b). The power output from a 1 kW FPV was initially calculated at hourly intervals and then

summed annually. These summaries represent the average annual sum over the period 1991–2020. The median surface area for each water body was calculated from monthly reconstructions that were based on a satellite-derived water surface area time series.

(Supplementary Fig. 1). Assuming a 1 kW FPV system, we simulated daily electricity outputs for each of the ~1 million water bodies using the Global Solar Energy Estimator (GSEE) tool<sup>10</sup>, based on climate input data from ERA5, the European Centre for Medium-Range Weather Forecasts' fifth generation atmospheric reanalysis of the global climate<sup>11</sup> (Methods). We then calculated the total annual power output for each water body by multiplying the 1 kW FPV annual power output by an area equivalent to 10% of the median surface area of each water body during the study period (1991–2020) (Methods). Although the percent surface coverage of FPVs can vary widely across host water bodies, with literature values ranging from less than 1% to more than 90% (ref. 12), we follow a conservative approach and consider 10% coverage (up to 30 km<sup>2</sup>; Methods) for all sites<sup>7</sup>.

### The theoretical global potential for FPVs

Considering a 1 kW FPV, we calculated a total global annual power output of 1,301 GWh (Fig. 1a) across the ~1 million water bodies. There were clear spatial patterns in power output, at both annual and monthly time-scales (Fig. 1 and Supplementary Fig. 2, respectively), largely reflecting geographical variations in solar irradiance due to differences in latitude, altitude and cloud cover (Supplementary Fig. 3). The simulated annual power output varied, per water body, from less than 1,250 kWh in, for example, northern Europe, to more than 2,500 kWh in regions such as the western United States, the Andean Mountains in South America and the Qinghai–Tibet Plateau in Asia (Fig. 1). Moreover, the simulated annual capacity factor, which is the proportion of maximum capacity

per year from a FPV and an indicator of economic viability, varied from a minimum of 10–15% in many European countries situated at latitudes above 48° N (for example, 12% in the United Kingdom) to more than 30% in the regions mentioned above with the highest power output (Supplementary Fig. 4). Our calculations suggest clear seasonal patterns in the simulated capacity factor, for example, varying from less than 7.5% to more than 20% across the Northern Hemisphere during boreal winter (December–February) and summer (June–August), respectively (Supplementary Fig. 5).

Globally, we calculated a total theoretical annual power output of 14,906 TWh across the ~1 million water bodies when considering a 10% surface coverage of FPV (up to 30 km<sup>2</sup>). In addition to being influenced by geographical variations in solar irradiance, the total power output from each water body will be influenced by the area of water available to host FPVs. Intuitively, larger water bodies can host larger FPV arrays given a specific percent area coverage. Following the methods outlined in ref. 13, here we reconstructed the monthly water surface area time series for each of the ~1 million water bodies from 1991 to 2020 (Methods). Our analysis demonstrates clear geographical variations in water body surface area during the study period (Fig. 1b). We demonstrate that some parts of the world are dominated by the presence of small water bodies (<0.5 km<sup>2</sup>), such as some regions in northwestern Canada, the western United States and eastern South America, whereas others are dominated by the presence of larger water bodies (>20 km<sup>2</sup>), such as the northeastern United States (Fig. 1b). By multiplying the power output of a single FPV with 10% of the water body surface area

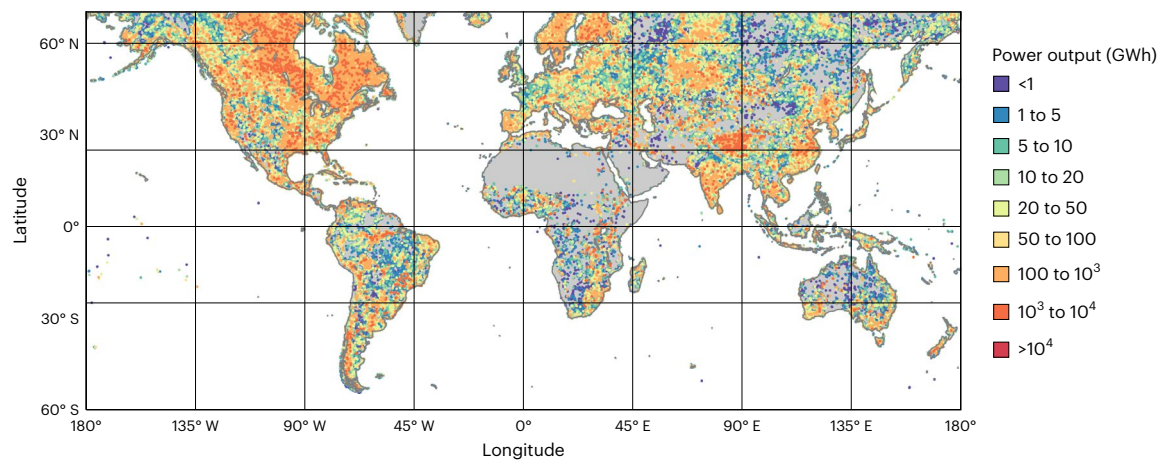


**Fig. 2 | The theoretical global potential for FPV.** Shown, for each of the >1 million water bodies considered in this study, is the total annual power output of a FPV system when 10% of the water body surface area (up to 30 km<sup>2</sup>) is occupied.

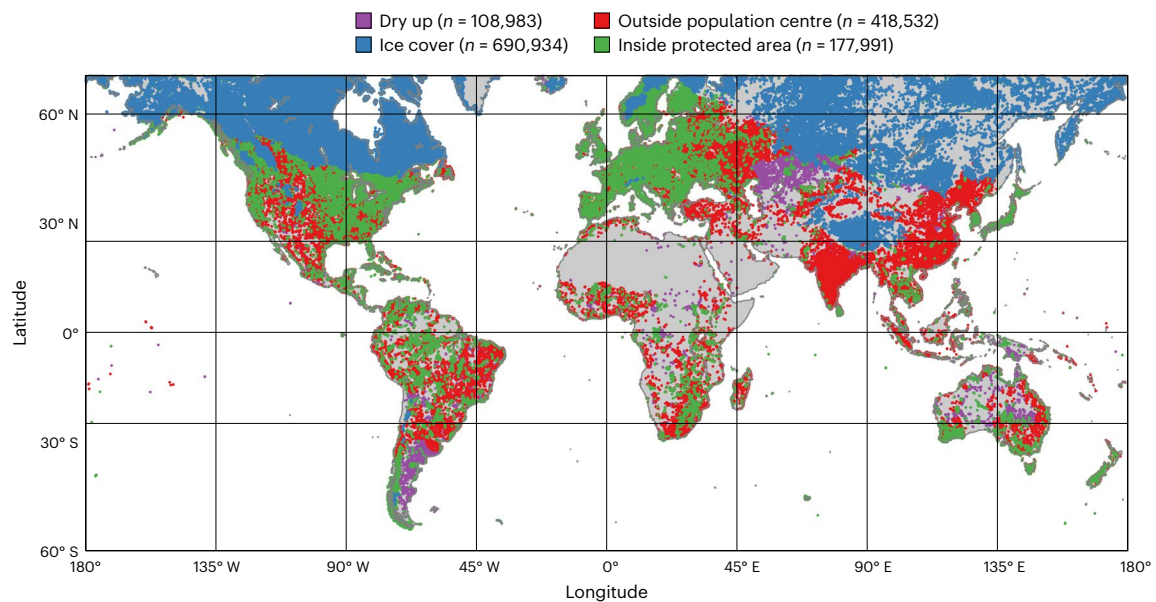


**Fig. 3 | Water body constraints on global FPV potential.** Shown are the location of each water body that we consider unfeasible for FPV deployment. The water body constraints that we consider in this study include the distance from each water body to a population centre (>10 km), water bodies that are situated inside protected areas, when the annual fraction of ice cover exceeds 50% (that is, the typical annual ice cover fraction from 1991 to 2020) and those that have dried up during the study period. Note that some lakes meet the criteria for more than

one constraint, for example, those situated within a protected area and outside a population centre. Thus, the values shown in the legend do not add up to the total number of water bodies included in this study. To best visualize these results, we shifted the latitude and longitude of water bodies randomly by  $\pm 0.05^\circ$  when plotting the different constraints. However, some points on the map are still overlapping.

(up to 30 km<sup>2</sup>), we estimate a theoretical total power output for each of the ~1 million water bodies considered in this study (Fig. 2). Our simulations demonstrate considerable differences in the total theoretical annual power output by FPV, which differ by several orders of magnitude worldwide (Fig. 2).

### Water body constraints on global FPV potential

The theoretical global analysis described above considered that all ~1 million water bodies included in our dataset were suitable to host FPVs. However, there are several factors that must be considered when selecting appropriate water bodies for this renewable energy technology (Fig. 3). The key constraints we include for a water body are (1) it is located within 10 km of a population centre; (2) it is not situated within a protected area; (3) the duration of ice cover is less than six months and (4) the water body has not dried up during the study period

(for example, Supplementary Fig. 6) (Methods). After selecting sites that we considered suitable to host FPVs based on these constraints, a total of 67,893 water bodies remained in our global dataset (that is, 94% of the studied water bodies were unsuitable according to our criteria). For each of the water bodies that remained, we re-calculated the total power output from FPV. Specifically, by applying a similar approach to our theoretical global analysis, we considered a 1 kW FPV and calculated the total annual power output from each water body assuming a 10% surface cover (up to 30 km<sup>2</sup>). Globally, we estimated a total annual power output of 1,302 TWh across all 67,893 water bodies. A considerable fraction of the global power output from FPV would be generated from water bodies located within specific countries (Supplementary Table 1), including large ones such as China (252 TWh), Brazil (170 TWh) and the United States (153 TWh). However, we also find that some comparatively smaller countries can produce a considerable



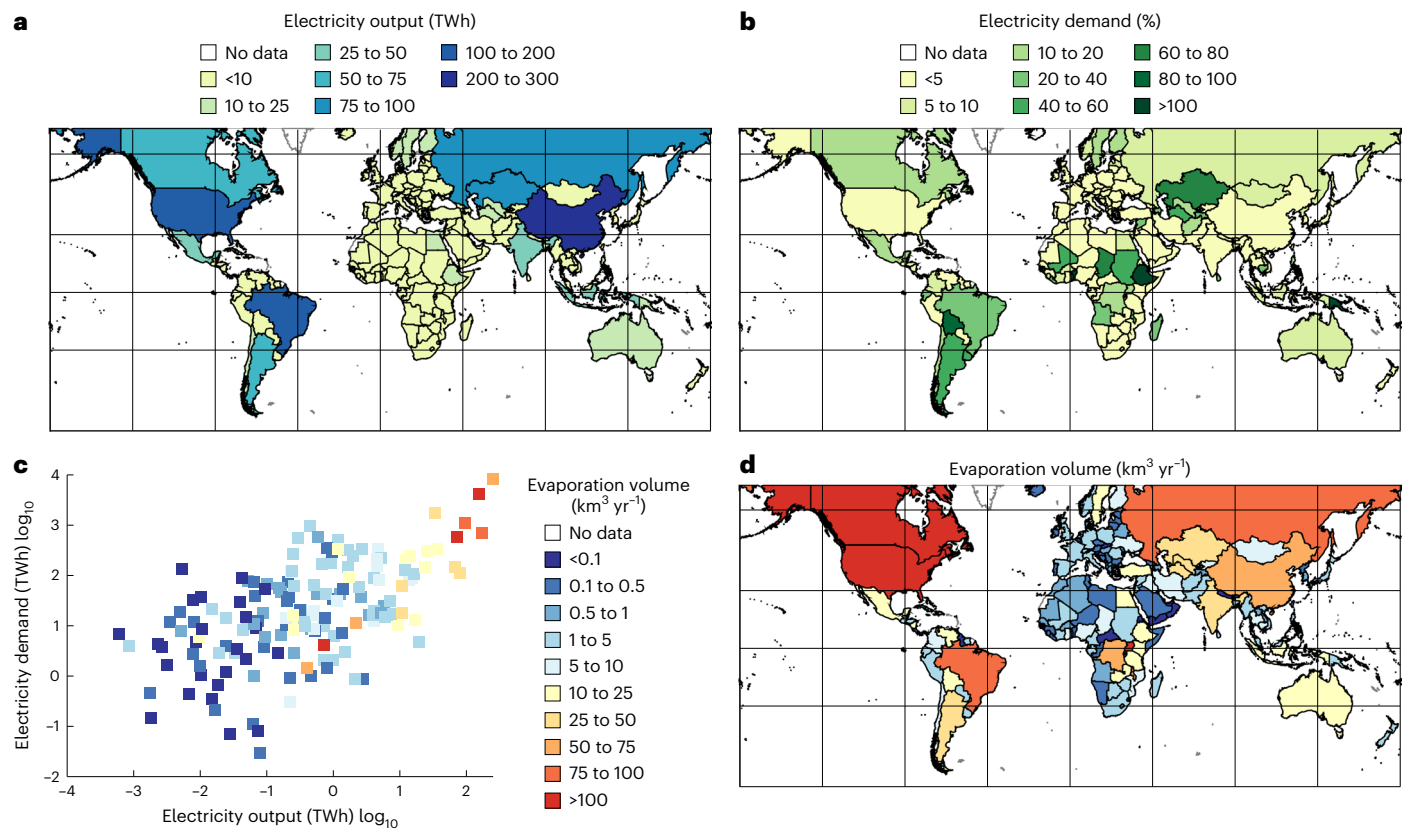


**Fig. 4 | National-scale summaries of FPV potential and water loss via evaporation. a, b.** Shown are the simulated total annual power output when 10% of the surface area of all suitable water bodies are occupied by FPV (a) and the

percentage of total electricity demand met by FPV in each country (b). c. The relationship among the power output by FPV, electricity demand and sum of water loss via evaporation per country. d. Water loss via evaporation per country.

amount of electricity from FPV. For example, the country with the 12th largest estimated total power output from FPV, within this feasibility study, was Papua New Guinea (19 TWh), which is not only located near the equator where solar irradiance is high (Supplementary Fig. 3) but is also home to some large water bodies, such as Lake Murray (647 km<sup>2</sup>) and Lake Kutubu (49 km<sup>2</sup>).

## Potential for FPV to decarbonize national economies

Our estimates suggest that FPV could play an important role in meeting the energy demands of several countries and aid in decarbonizing the economy. By summarizing our results at the country level, we provide estimates of national-scale total FPV power outputs worldwide (Fig. 4a) and calculate the percentage of national electricity demand it would meet (Fig. 4b and Supplementary Fig. 7). We estimate that if all water bodies that we consider feasible have 10% of their surface area covered by FPVs (up to 30 km<sup>2</sup>), a few countries considered in this study (approximately 3%) could meet their energy demand via this renewable energy technology (Supplementary Table 1). For some countries, for example, Bolivia, FPV production (9 TWh) almost meets demand (11 TWh in 2021), whereas in others it either exceeds, for example, Ethiopia (129% of electricity demand from FPV), or falls short but still makes a valuable contribution, for example, Finland (17% of electricity demand from FPV). However, for some nations, there is limited potential suggesting it is not a viable means to decarbonize the economy but can still provide a valuable source of renewable energy. On average, across all countries, the percent of electricity demand that could be met by FPV is 16% (Supplementary Table 1). Moreover, our analysis suggests that the countries with the greatest total power output from FPVs are typically those with the greatest electricity demand (Fig. 4c).

The decarbonization potential of FPV could be especially important for national economies currently powered by high carbon intensity electricity (Supplementary Fig. 8). We find that some of the countries with high FPV potential, such as China, also have a high carbon intensity of electricity (544 g CO<sub>2</sub>e (Carbon dioxide equivalent) in 2021). Crucially, FPV could also increase access to electricity to communities in some nations (Supplementary Fig. 9). For example, in Chad or Malawi, where the installation of FPVs in selected water bodies could contribute substantially to national electricity demand (73% and 29%, respectively); approximately one-tenth of the population of these countries do not have access to electricity (Supplementary Table 1). Thus, as a low carbon source of electricity, FPV could be a useful tool to provide electricity to these regions and others. However, it is also important to note that in many regions (for example, sub-Saharan Africa), it is not simply a question of electricity supply but also connection, which can be difficult. We also calculated the potential reduction in total CO<sub>2</sub> emissions, which could be achieved following the deployment of FPV in each country (Methods). By replacing a percentage of the total electricity demand with what could be met by FPV and considering their own estimated carbon intensity, we calculated variable reductions in national CO<sub>2</sub> emissions (Supplementary Fig. 10 and Supplementary Table 1). For example, we estimated an annual (in 2021) decrease of 0.13 billion tonnes of CO<sub>2</sub> in China and 0.05 billion tonnes of CO<sub>2</sub> in the United States, two of the world's largest emitters in 2021, despite FPVs meeting only 3% and 4% of energy demand. Globally, the deployment of FPVs could lead to a total annual reduction of 0.45 billion tonnes of CO<sub>2</sub> (in 2021). However, we also find that in some countries where the carbon intensity of electricity is already very low (for example, Paraguay ≈ 25 g CO<sub>2</sub> kWh<sup>-1</sup>), our calculations suggest a negative impact of FPV on total CO<sub>2</sub> emissions (that is, leading to higher CO<sub>2</sub>). Additionally, for nations whose energy supply is dominated by hydro and wind,

FPVs may increase CO<sub>2</sub> emissions given PVs' higher carbon intensity. However, as with any estimates relating to a relatively new technology, we are aware that FPV is still maturing, with limited studies on the embedded carbon intensity (Methods), and these could be misleading given local conditions and design variations that will influence their carbon intensity. There are also unknown impacts of FPVs on water body carbon cycling and their knock-on impacts on, among other things, CO<sub>2</sub> emissions from water bodies. Lastly, the total reduction in CO<sub>2</sub> emissions that we calculated are influenced by the water body constraints that we previously defined. These estimates can vary depending on the number of water bodies included in any national-scale or global analysis.

Whereas our numerical modelling approach provides important new insights on FPV potential worldwide, it is important to consider that our chosen thresholds for key constraining factors could be defined differently depending on specific use cases. We therefore encourage those interested in assessing local–regional potential to modify the thresholds we imposed using the information that we provide (Data availability).

### Potential for FPV to reduce water scarcity

Water is a critical resource, underpinning the provision of many ecosystem services required by society. However, in some regions supply is increasingly scarce given demand and the impact of climate change. FPV technologies have the potential to reduce water scarcity mitigating water loss via evaporation, which is accelerating globally under climate change<sup>13–16</sup>. Indeed, FPV systems are emerging as a potential mitigation strategy for water scarcity by reducing evaporative water loss from reservoirs and lakes in many parts of the world<sup>14,17–22</sup>, corroborated by numerous studies. FPVs probably exert a dual influence on evaporation rates. First, they create a shading effect, decreasing water surface temperature and consequently suppressing the vapour pressure gradient at the air–water interface, a key driver of latent heat fluxes and, in turn, evaporation<sup>23–25</sup>. Second, FPVs may act as wind barriers, further dampening evaporative losses, as wind speed is positively correlated with evaporation rates<sup>26,27</sup>. The deployment of FPVs has the potential to reduce evaporative water loss, thereby contributing to the maintenance of water levels in water bodies and alleviating pressure on freshwater resources. To ensure a comprehensive evaluation, potential trade-offs and feedback loops must be considered. This also includes the influence of FPVs on local microclimates, an effect observed in land-based systems<sup>28,29</sup> and potentially applicable to large-scale FPV deployments. Following the methods of ref. 13, we estimated the total water loss via evaporation in each of the studied water bodies during the study period (Supplementary Fig. 11), and for each country, we calculated the total evaporative water loss. For example, the total annual water loss via evaporation in all studied water bodies in Canada and the United States was 230 km<sup>3</sup> and 221 km<sup>3</sup>, respectively (Fig. 4d). These are more than two orders of magnitude greater than calculated for many European, African and Asian countries. Moreover, we compare the geographical patterns in total evaporation volume and the total power output from FPV (Fig. 4c). We find that the countries with the greatest potential for FPV (that is, in terms of the power generated) are also those that experience the highest evaporative losses (Fig. 4c,d). Furthermore, in countries where the total volume of water lost via evaporation is low, including many central European countries, the total power output by FPV (and the percent of energy demand that FPVs can produce) is also comparatively little. This quantitative analysis thus highlights the combined benefit of installing FPVs in these countries, that is, to both help meet electricity demand and address water scarcity.

Furthermore, recent studies have suggested that FPVs could help mitigate the occurrence of algal blooms<sup>30,31</sup>, which have increased in many<sup>32</sup>, but not all<sup>33–36</sup>, inland water bodies in recent decades. This has implications for water availability and ecosystem function, as algal blooms are among some of the main causes of poor water quality and

can lead to serious health issues<sup>37–42</sup>. FPVs present a promising approach to water quality management, particularly in addressing algal bloom dynamics. These systems create a shading effect that directly reduces light availability, a critical factor limiting the growth of algae, which are predominantly photosynthetic organisms. Additionally, FPVs have the potential to disrupt water circulation patterns within the aquatic environment, thereby altering nutrient dynamics and influencing the availability of essential nutrients necessary for algal proliferation<sup>43–45</sup>. Whereas the precise magnitude of algal bloom reduction attributed to FPVs requires further investigation, initial studies suggest a compelling avenue for future research<sup>46–48</sup>. Quantifying the percentage reduction in algal blooms across a range of water body types and algal communities will be essential to ascertain the efficacy of FPVs as a water quality management tool. Such efforts hold promise in advancing our understanding of FPV-mediated interventions in aquatic ecosystems and their role in promoting sustainable water resource management practices.

By exploring the satellite-derived global algal bloom dataset of ref. 32, which includes information on algal bloom occurrence in 236,913 water bodies worldwide, we investigated the frequency of algal blooms during the study period (Supplementary Fig. 12a). Specifically, we calculated the percentage of water bodies with available data in each country that experienced an algal bloom (Supplementary Fig. 12b) and how frequently they have occurred (Supplementary Fig. 12c). Moreover, we compared the geographical patterns in algal bloom frequency with the total power output from FPV (Supplementary Table 1). We find no clear relationship between countries with the greatest potential for FPV (that is, in terms of the power generated) and those that experience the highest frequency of algal blooms (Supplementary Table 1). However, for some countries, FPV could be beneficial in terms of mitigating negative impacts of algal blooms. Using an algal bloom frequency of greater than 10% as a threshold (10% is considered high following ref. 32), there are many countries/water bodies that could benefit from FPV installation, with several also notably benefiting from the electricity production. For example, in Argentina where the installation of FPV in selected water bodies could produce sufficient energy to meet 45% (67 TWh) of the national electricity demand (149 TWh in 2021), the percentage of sites with available data that experience algal blooms is 11%. Similarly, during the same time period, 17% of water bodies with available data in Brazil have experienced an algal bloom, while also providing the potential to meet one quarter (170 TWh) of the electricity demand (686 TWh in 2021) of the country. Moreover, in Portugal where FPV could contribute over 3% of electricity demand, 30% of sites with available data have experienced algal blooms, the average frequency of which is 11%. Other country-level summaries are provided in Supplementary Table 1. However, we note that more research is needed to develop a mechanistic understanding of FPV impacts on algal blooms.

### Benefits, risks and unknowns of FPV deployment

FPV can provide higher power outputs while reducing land-use pressure and water scarcity when compared to other means of PV deployment. Moreover, our global estimate of FPV potential demonstrates the electricity supply benefit of this renewable energy technology. However, we lack a great deal of essential knowledge of the most likely impacts of FPV on hosting water bodies<sup>30,31,43,49–53</sup>. FPV could alter physical, biological and chemical states and processes within lakes and reservoirs, but it is challenging to forecast emergent ecosystem-level effects that arise from complex interactions within each water body and to then make generalizable predictions<sup>54</sup>. Nevertheless, existing site-specific studies, including those focusing on natural water surface coverings (for example, ice and floating-leaved vegetation), allow us to make tentative inferences of some of the probable impacts, which should be considered before a wider uptake of FPV.

Ecosystem impacts of FPV will be largely mediated through effects on physical states and processes<sup>54</sup>. Specifically, installations will

(1) reduce the amount of solar radiation reaching the water surface and (2) shelter the water body from the wind. These changes would have opposing effects on surface temperature, vertical mixing and therefore water body thermal structure. Consequently, it is currently unclear whether FPV will increase or decrease surface water temperature and water body mixing. These uncertainties over the physical effects of FPVs are of concern, given their regulation of biogeochemical cycles linked to eutrophication and ecosystem states and processes. Indeed, the installation of FPV is likely to have effects that cascade through the whole ecosystem, but unless the implications for physical attributes are resolved, there will be uncertainties over the direction and magnitude of broader responses. For example, water temperature and stratification influence dissolved oxygen concentrations in deep waters<sup>55</sup>, with cascading effects on nutrient release from sediments<sup>56,57</sup> and subsequent phytoplankton growth, the production of greenhouse gases such as methane<sup>58,59</sup> and nitrogen cycling<sup>60</sup>. Through shading, we would also expect FPV to impact upon the growth and composition of phytoplankton communities with knock-on impacts on the aquatic food web<sup>31,47,48,61</sup>.

Advancements in understanding of the complex impacts of FPVs on their host water bodies are mainly developed through modelling studies, either via mesocosm experiments<sup>46,47,61–64</sup> or computational assessments<sup>18–22,48,65</sup>. Most research to date focuses on the potential water savings that come from FPV deployment depending on the surface coverage. Far fewer assessments of hydrodynamic or water quality impacts exist. We must rapidly accelerate knowledge of these physical and biogeochemical impacts to ensure that the pathway to decarbonization continues while minimizing concomitant environmental impacts and that low carbon electricity generation is not exploited at the cost of other essential ecosystem services that fresh waters provide to society (biodiversity, drinking water, fisheries, hydropower, irrigation of crops).

It is imperative to carefully consider the ecological implications and trade-offs associated with each potential FPV deployment. Whereas FPV presents a promising avenue for decarbonization, its deployment on natural lakes could pose considerable risks to freshwater ecosystems and native biodiversity, which is increasingly at risk from external pressures<sup>66,67</sup>. As such, any proposal to utilize natural lakes for FPV installations must be accompanied by comprehensive environmental and ecological impact assessments, stakeholder consultations and adherence to robust regulatory frameworks. Moreover, given the sensitivity of pristine natural lakes and the potential for irreversible ecological damage, caution must be exercised in targeting such ecosystems for FPV deployment. Future research efforts should prioritize investigating and building a predictive understanding of the ecological consequences of FPV on freshwater systems, and this knowledge must be used to develop strategies to mitigate potential negative impacts while maximizing the co-benefits of this technology. By integrating environmental considerations into decision-making processes and adopting a precautionary approach, we can ensure that FPV deployment on natural lakes contributes to sustainable development goals while safeguarding freshwater ecosystems for future generations. In addition, whereas our analysis removed lakes within protected areas, it is important to recognize that thousands of critically important natural lakes exist in areas that are not formally categorized as protected. These ecosystems are often vulnerable to anthropogenic disturbances and face increasing pressures from various human activities, including infrastructure development. Therefore, any proposal to deploy FPV on natural lakes must consider the unique ecological characteristics and conservation status of each site and seek to minimize impacts through design decisions and mitigation measures, even if those sites are not within formally designated protected areas. This underscores the need for a nuanced approach that balances the potential benefits of FPV deployment with the imperative to preserve the ecological integrity of freshwater ecosystems.

## Pathway to judicious FPV deployment

Considering the concerns described above regarding the potential environmental impacts of installing FPVs, developing modelling capabilities and decision support tools to guide deployment location (both between and within water bodies), FPV design and extent and any desirable management (that is, water body mixing or aerating) would promote sustainable deployment of FPV. Without such capabilities it might be desirable to begin this transition to low carbon energy generation by focusing on artificially created water bodies<sup>7,8</sup>. One could argue that there might be greater environmental concerns associated with natural water bodies than artificial ones and, as the latter are often already managed, installing FPVs is likely to be more straightforward because of the presence of existing infrastructure<sup>68</sup>. Moreover, it is critical to consider societal values of potential deployment sites, as for all renewable energy infrastructure<sup>63</sup>.

From a technical standpoint, installing FPV on hydroelectric reservoirs can optimize energy efficiency and improve system reliability<sup>50,69</sup>. Integrated hydroelectric–FPV systems may also lessen the environmental and social impacts of standalone hydroelectric operation<sup>70</sup> providing synergistic benefits to the water–food–energy nexus<sup>69</sup>. However, it is important to consider that whereas some infrastructure is already in place in hydroelectric reservoirs, they might already be operating at full operational capacity, meaning that systems will need to be updated to receive additional power from FPV. Another important technological consideration for the installation of FPVs, not only in artificial reservoirs but also in natural lakes worldwide, is the material required to support a wider uptake of renewable energy technology<sup>71</sup> and the need to transport those materials to specific water bodies, which can be problematic. We also note that the potential biodiversity value of artificial water bodies<sup>72</sup> means that plans to develop FPVs on anthropogenic fresh waters do not obviate the need for thorough consideration of ecological impacts.

## Methods

### Study sites

In this project, we investigated the FPV potential of over 1 million (1,050,251) globally distributed water bodies (>0.1 km<sup>2</sup> in surface area), the location (and shapefiles) of which were extracted from the HydroLAKES database<sup>73</sup>. This global dataset of water body characteristics also includes information on 6,673 reservoirs based on the Global Reservoir and Dam database<sup>74</sup>.

### Global simulation of FPV power output

For each of the ~1 million water bodies investigated in this study, we used the Global Solar Energy Estimator (GSEE)<sup>10</sup> to simulate the PV power output at hourly resolution from 1991 to 2020. GSEE requires as input specific information on the PV modules, including their capacity and tilt angle and hourly data for solar irradiance (direct and diffuse) and air temperature. In this project, climate data were downloaded from the ERA5 (available at 0.25° longitude–latitude resolution) reanalysis product<sup>11</sup>. Notably, the grid cell climate forcing from ERA5 was used to represent conditions for a specific lake location within the global simulations. In this study, we assumed that the FPV had a capacity of 1 kW, and we set the tilt angle to the latitude of the water body when situated between 0° and 15° N/S and to 15° elsewhere. This follows the recommendation of the World Bank FPV practitioner's handbook<sup>75</sup>, resulting in high-density arrangements. Higher tilt angles are generally not deployed in FPV settings due to concerns about wind loading, shading that would occur from densely packed panels and increased material costs that would rise from installing at higher angles. We also assumed fixed-tilt rigging, which is reasonable for a global-scale assessment. FPVs can also be one- or two-axis tracking, which intuitively would result in greater power output. Thus, here we follow a conservative approach, and the current most popular deployment means, and assume fixed FPVs. Considering that FPVs are up to 10% more



efficient than land-based solar PV<sup>5,6,76–78</sup>, for which GSEE was developed, we adjusted the GSEE outputs accordingly. However, the efficiency increases of FPVs compared with land-based ones can be higher<sup>51</sup>. Once we simulated the power output for a 1 kW FPV in each water body, we then upscaled these estimates based on a surface area that was equal to 10% of the water body surface area (below). Specifically, by assuming an FPV footprint of 10 m<sup>2</sup> kW<sup>-1</sup>, we could estimate how many panels could be installed per lake to occupy 10% of the water surface area (up to 30 km<sup>2</sup>; below) and multiply our annual power output accordingly. A footprint of 10 m<sup>2</sup> kW<sup>-1</sup> was selected as it can be scaled with ease and the footprints of six sampled FPV systems (Queen Elizabeth II, United Kingdom; Langthwaite Reservoir, United Kingdom, and four US systems detailed in ref. 3) ranged from 7.2 to 15.3 m<sup>2</sup> kW<sup>-1</sup>. Whereas FPVs can be deployed at a range of coverage depending on, among other things, the design of the FPV (for example, tilt angle) and the rated capacity of the installation, here we follow a conservative approach and consider 10% coverage for all sites. We highlight that PV power outputs from GSEE using reanalysis input data have been validated previously against metered time series from more than 1,000 PVs<sup>10</sup>. We also considered the potential technical constraints related to the total size of an FPV array. In this study, we follow ref. 8 and impose a maximum coverage area of any one system to 30 km<sup>2</sup>. This threshold is based on one of the largest FPV systems in the world, which is located at the Saemangeum site in the Yellow Sea off Korea<sup>79</sup>. We do note, however, that there is the potential for larger systems, such as the Bhadla Solar Park located in the Thar Desert of Rajasthan, India, which covers an area of 56 km<sup>2</sup> and has a total installed capacity of 2,245 MW. We anticipate that the maximum footprint of these systems will also increase in the future.

### Water body constraints on FPV

There are several factors that must be considered when selecting appropriate water bodies for this renewable energy technology. The key constraints that we considered in our study included (1) it is located within 10 km of a population centre; (2) it is not situated within a protected area; (3) the duration of ice cover is less than six months and (4) the water body has not dried up during the study period. The distance to the population centre has been selected as a distance for which it is likely to lay a transmission line, either to the load centre or to connect to a grid via more proximal existing transmission lines. Some previous national-scale studies have considered 80 km from a transmission line as a feasible distance for deploying FPVs<sup>12</sup>. Thus, we consider our analysis conservative in terms of the number of lakes included in our feasibility study. The presence of ice can make it difficult to not only install FPV but can also damage FPV installations by influencing buoyancy and overall load, that is, ice can be detrimental for FPV by imposing high loads on the mooring system. Extremely cold areas are also often accompanied by high snow loads, reducing electricity generation if the array is covered and special anchoring materials and higher project cost compared to conventional FPV projects. In terms of variations in water body surface area and, in turn, water depth, water bodies that dry up could be considered unfavourable given additional costs associated with mooring/anchorage—as suggested in the World Bank FPV practitioner's handbook<sup>75</sup>—and the reduced efficiency of FPVs when they are not displaced on water. Critically, there is a potential issue of FPVs becoming stranded if a shallow water body dries up temporarily, as can occur in many water bodies worldwide<sup>1</sup>. However, with all these constraints, their global applicability will depend on local specifics. For example, it may be cost effective to connect a very large FPV system to a transmission line or load centre >10 km away. Moreover, any increased costs associated with greater transmission distances, cold environments and variable water surface areas need to be placed in the context of alternative sources of low carbon electricity. Thus, whereas our study outlines key constraints and selection criteria for identifying suitable water bodies, we acknowledge that the global applicability of these criteria is contingent upon local specifics and

associated costs. Factors such as local climate conditions, regulatory frameworks, economic feasibility, environmental impacts and social acceptance all play important roles in determining the feasibility and success of FPV projects. Recognizing this complexity, we advocate for a comprehensive analysis that integrates technical, economic, environmental and social dimensions into the decision-making process. We provide the calculated FPV outputs for each of the ~1 million water bodies included in this study, allowing the water body constraints described above to be modified according to user requirements (Data availability). In turn, the results that we present in our feasibility study, which are based largely on our own evaluation and experience, will differ if these constraints are altered.

### Water body surface area

To calculate the surface area of each water body in this study (1991–2020), we followed the methods outlined in ref. 13. In brief, we reconstructed the monthly water surface area time series for the >1 million lakes based on a combination of the dynamic Landsat-based global surface water (GSW) dataset<sup>80</sup> and the static HydroLAKES shapefiles<sup>73</sup>. For each month and each water body, the water classification map from the GSW dataset is extracted within the defined boundary of the HydroLAKES shapefiles. However, such water classification maps are frequently contaminated by cloud cover, cloud shadow and sensor failure, leading to large data gaps. Here we adopted the automatic image enhancement algorithm from ref. 13, which detects the 'observable' water edge and extends it to the 'contaminated' area according to the water occurrence image, to create the complete water surface (Supplementary Fig. 13). Then the surface area time series at a monthly time step from 1991 to 2020 for each lake is constructed. For new reservoirs that were built after 1991, we calculated surface area variations from five years after the construction year.

### Information on electricity demand, carbon intensity of electricity and electricity access

We downloaded information on national-scale annual electricity demand, carbon intensity of electricity and the percentage of the population that has access to it from ref. 81. Electricity demand is described as total electricity generation, adjusted for electricity imports and exports. Carbon intensity is measured in grams of carbon dioxide equivalents emitted per kilowatt-hour of electricity. Access to electricity is defined as having an electricity source that can provide very basic lighting and charge a phone or power a radio for 4 hours per day. For each of these metrics, we used the latest annual information available. This includes data from 2021 for both annual electricity demand and its carbon intensity and data from 2020 for electricity access. For consistency, we do not include data from different years when investigating global patterns in each metric. For example, in terms of energy demand, some countries (for example, Albania, Iceland) did not have information for 2021 (only 2020) and thus were not included in the analysis.

We also calculated the potential reduction in total CO<sub>2</sub> emissions following the deployment of FPV. To achieve this, we first calculated the total annual CO<sub>2</sub> emissions per country by multiplying the electricity demand with its carbon intensity<sup>81</sup>. We then calculated the total annual CO<sub>2</sub> emissions that would be reduced if a percentage of the total energy demand was met by FPV, that is, if they were deployed on the water bodies that we considered feasible. There is no definitive carbon intensity value for FPV given the relative immaturity of the deployment means and variations due to design, location and where components are sourced from. Consequently, we used the IPCC (Intergovernmental Panel on Climate Change) life-cycle CO<sub>2</sub>e emissions per kWh produced by rooftop PVs, which are approximately 41 g CO<sub>2</sub> kWh<sup>-1</sup> (ref. 82), to estimate the total annual CO<sub>2</sub> emissions associated with FPVs. Using these estimates, we calculated the potential reduction in total CO<sub>2</sub> emissions in each country (Supplementary Table 1).

### Proximity of water body to a population centre

When selecting a water body suitable for FPVs, we considered their proximity to a population centre, which we use in this study as a proxy for distance to a transmission line or a load centre. Specifically, we only considered water bodies that were located within 10 km of a population centre as feasible for the installation of FPV. Here we define a population centre as a region with a population of at least 1,000 people and a population density of  $\geq 400$  people per square kilometre. Population data were extracted from the Socioeconomic Data and Applications Center<sup>83</sup>, available at a 30 arcsecond spatial resolution. Lakes situated within 10 km of a population centre were considered suitable for FPV.

### Protected areas

Information on the location of protected areas was extracted from the World Database on Protected Areas<sup>84</sup>. In this study, we considered a water body to be located within a protected area where the water body polygon intersected with a protected area polygon. However, this is a conservative approach to accounting for ecological impact, as many fresh waters with great biodiversity value exist outside of the current protected area network<sup>85</sup>.

### Water loss by evaporation

To estimate the volume of water lost via evaporation in each of our studied sites, we followed the methods outlined in ref. 86. Specifically, the monthly evaporation rate was calculated for each lake using the Penman equation by considering the heat storage effect (equation (1)). We used the average evaporation rate derived based on three meteorological forcing datasets (that is, TerraClimate, ERA5 and GLDAS) to take account of forcing data uncertainty. The evaporation rate was estimated as:

$$E = (\Delta(R_n - G) + \gamma f(u)(e_s - e_a)) / (\lambda_v(\Delta + \gamma)) \quad (1)$$

where  $E$  is the open water evaporation rate ( $\text{mm d}^{-1}$ );  $\Delta$  is the slope of the saturation vapour pressure curve ( $\text{kPa } ^\circ\text{C}^{-1}$ );  $R_n$  is the net radiation ( $\text{MJ m}^{-2} \text{d}^{-1}$ );  $G$  is the heat storage change of the water body ( $\text{MJ m}^{-2} \text{d}^{-1}$ );  $\gamma$  is the psychrometric constant ( $\text{kPa } ^\circ\text{C}^{-1}$ );  $f(u)$  is the wind function and is equal to  $\lambda_v(2.33 + 1.65 u) L_f^{-0.1}$  ( $\text{MJ m}^{-2} \text{d}^{-1} \text{kPa}^{-1}$ );  $L_f$  is the average lake fetch at the wind direction (m);  $e_s$  is the saturated vapour pressure at air temperature (kPa);  $e_a$  is the air vapour pressure (kPa); and  $\lambda_v$  is the latent heat of vapourization ( $\text{MJ kg}^{-1}$ ). Then the volumetric water losses via evaporation for each lake were estimated by multiplying the evaporation rate and the water body surface area.

### Ice cover duration

To determine the duration of ice cover in each of the studied water bodies, we used an air temperature-based approach<sup>13</sup>. Instead of the simple  $0^\circ\text{C}$  isothermal approach, we specifically modelled (1) the freeze time lag, which is the time difference between the date when the air temperature drops to zero and the lake freezing date and (2) the thaw time lag which is the time difference between the date when the air temperature rises back to zero and the lake thaw date (Supplementary Fig. 14). The freeze time lag is caused by the higher specific heat capacity of water than air and thus water temperature cools at a slower rate than the air temperature, whereas the thaw time lag is caused by the thickness of lake ice that has been accumulated during the previous winter. Considering both time lags, the total ice cover duration for a lake ( $D_{\text{ice}}$ ) is calculated following equation (2)

$$D_{\text{ice}} = D_{\text{total}} - \text{Lag}_{\text{freeze}} + \text{Lag}_{\text{thaw}} \quad (2)$$

where  $D_{\text{ice}}$  is the lake ice duration in days for each month;  $D_{\text{total}}$  is the total lake ice duration in days for each month based on the  $0^\circ\text{C}$  isothermal approach;  $\text{Lag}_{\text{freeze}}$  is freeze lag in days; and  $\text{Lag}_{\text{thaw}}$  is the thaw lag in days.

### Algal bloom occurrence

To investigate the occurrence and frequency of algal blooms in water bodies worldwide, we explored the satellite-derived global bloom dataset of ref. 32. Approximately 17% of the ~1 million water bodies investigated in this study ( $n = 236,913$ ) were included in the global bloom dataset, with the remainder considered unfeasible, primarily due to relatively high uncertainty in algal bloom detection via Landsat imagery<sup>32</sup>. For the water bodies considered suitable, ref. 32 investigated data related to the occurrence frequency of algal blooms, defined as the ratio between the number of detected algal blooms to the number of valid satellite observations within the period of interest (1982–2019). In this study, we used this dataset to calculate two key metrics: (1) the percentage of lakes within a country that have experienced at least one algal bloom and (2) in lakes where algal blooms have been observed, we calculate a country-level average frequency of occurrence.

### Data availability

ERA5 solar radiation and air temperature data used in this study are available at <https://cds.climate.copernicus.eu/cdsapp#!/dataset/reanalysis-era5-single-levels?tab=overview>. Outputs from the Global Solar Energy Estimator for each of the studied lakes are available via Figshare (ref. 87).

### Code availability

Code used to run the Global Solar Energy Estimator is available via Github at <https://github.com/gzhaowater/fpvGSEE>.

### References

1. *Energy Transition Outlook 2022: A Global and Regional Forecast to 2050* (Det Norske Veritas, 2022); <https://www.dnv.com/energy-transition-outlook/index.html>
2. Cazzaniga, R. & Rosa-Clot, M. The booming of floating PV. *Sol. Energy* **219**, 3–10 (2021).
3. Cagle, A. E. et al. The land sparing, water surface use efficiency, and water surface transformation of floating photovoltaic solar energy installations. *Sustainability* **12**, 8154 (2020).
4. Farrar, L. W. et al. Floating solar PV to reduce water evaporation in water stressed regions and powering water pumping: case study Jordan. *Energy Convers. Manage.* **260**, 115598 (2022).
5. de Sacramento, E. M. et al. Scenarios for use of floating photovoltaic plants in Brazilian reservoirs. *IET Renewable Power Gener.* **9**, 1019–1024 (2015).
6. Liu, H. et al. Field experience and performance analysis of floating PV technologies in the tropics. *Prog. Photovoltaics Res. Appl.* **26**, 957–967 (2018).
7. Almeida, R. M. et al. Floating solar power could help fight climate change—let's get it right. *Nature* **606**, 246–249 (2022).
8. Jin, Y. et al. Energy production and water savings from floating solar photovoltaics on global reservoirs. *Nat. Sustain.* **25**, 105253 (2023).
9. Verpoorter, C., Kutser, T., Seekell, D. A. & Tranvik, L. J. A global inventory of lakes based on high-resolution satellite imagery. *Geophys. Res. Lett.* **41**, 6396–6402 (2014).
10. Pfenninger, S. & Staffell, I. Long-term patterns of European PV output using 30 years of validated hourly reanalysis and satellite data. *Energy* **114**, 1251–1265 (2016).
11. Hersbach, H. et al. The ERA5 global reanalysis. *Q. J. R. Meteorol. Soc.* **146**, 1999–2049 (2020).
12. Spencer, R. S. et al. Floating photovoltaic systems: assessing the technical potential of photovoltaic systems on man-made water bodies in the continental United States. *Environ. Sci. Technol.* **53**, 1680–1689 (2019).
13. Zhao, G. et al. Evaporative water loss of 1.42 million global lakes. *Nat. Commun.* **13**, 3686 (2022).



14. Wang, W. et al. Global lake evaporation accelerated by changes in surface energy allocation in a warmer climate. *Nat. Geosci.* **11**, 410–414 (2018).
15. Zhou, W. et al. Spatial pattern of lake evaporation increases under global warming linked to regional hydroclimate change. *Commun. Earth Environ.* **2**, 255 (2021).
16. La Fuente, S. et al. Ensemble modeling of global lake evaporation under climate change. *J. Hydrol.* **631**, 130647 (2024).
17. Lopes, M. P. C. et al. Water-energy nexus: floating photovoltaic systems promoting water security and energy generation in the semiarid region of Brasil. *J. Clean. Prod.* **273**, 122010 (2020).
18. Fereshtehpour, M. et al. Evaluation of factors governing the use of floating solar system: a study on Iran's important water infrastructures. *Renewable Energy* **171**, 1171–1187 (2021).
19. da Costa, L. C. A. & da Silva, G. D. P. Save water and energy: a techno-economic analysis of a floating solar photovoltaic system to power a water integration project in the Brazilian semiarid. *Int. J. Energy Res.* **45**, 17924–17941 (2021).
20. de Campos, E. F. et al. Hybrid power generation for increasing water and energy securities during drought: exploring local and regional effects in a semi-arid basin. *J. Environ. Manage.* **294**, 112989 (2021).
21. Agrawal, K. K. et al. Assessment of floating solar PV (FSPV) potential and water conservation: case study on Rajghat Dam in Uttar Pradesh, India. *Energy Sustain. Dev.* **66**, 287–295 (2022).
22. Ateş, A. M. Unlocking the floating photovoltaic potential of Türkiye's hydroelectric power plants. *Renewable Energy* **199**, 1495–1509 (2022).
23. Hostetler, S. & Bartlein, P. Simulation of lake evaporation with application to modelling lake level variations of Harney-Malheur Lake, Oregon. *Water Resour. Res.* **26**, 2603–2612 (1990).
24. Lenters, J. D., Kratz, T. K. & Bowser, C. J. Effects of climate variability on lake evaporation: results from a long-term energy budget study of Sparkling Lake, northern Wisconsin (USA). *J. Hydrol.* **308**, 168–195 (2005).
25. La Fuente, S. et al. Multi-model projections of future evaporation in a sub-tropical lake. *J. Hydrol.* **615**, 128729 (2022).
26. Rodrigues, I. S. et al. Trends of evaporation in Brazilian tropical reservoirs using remote sensing. *J. Hydrol.* **598**, 126473 (2021).
27. Rocha, S. M. G. et al. Assessment of total evaporation rates and its surface distribution by tridimensional modelling and remote sensing. *J. Environ. Manage.* **327**, 116846 (2023).
28. Wu, C. et al. Ecohydrological effects of photovoltaic solar farms on soil microclimates and moisture regimes in arid Northwest China: a modelling study. *Sci. Total Environ.* **802**, 149946 (2022).
29. Zheng, J. et al. An observational study on the microclimate and soil thermal regimes under solar photovoltaic arrays. *Sol. Energy* **266**, 112159 (2023).
30. Zhang, N. et al. High-performance semitransparent polymer solar cells floating on water: rational analysis of power generation, water evaporation and algal growth. *Nano Energy* **77**, 105111 (2020).
31. Exley, G. et al. Floating solar panels on reservoirs impact phytoplankton populations: a modelling experiment. *J. Environ. Manage.* **324**, 116410 (2022).
32. Hou, X. et al. Global mapping reveals increase in lacustrine algal blooms over the past decade. *Nat. Geosci.* **15**, 130–134 (2022).
33. Oliver, S. K. et al. Unexpected stasis in a changing world: lake nutrient and chlorophyll trends since 1990. *Glob. Change Biol.* **23**, 5455–5467 (2017).
34. Paltsev, A. & Creed, I. F. Are northern lakes in relatively intact temperate forests showing signs of increasing phytoplankton biomass? *Ecosystems* **25**, 727–755 (2021).
35. Topp, S. N. et al. Multi-decadal improvement in US lake water clarity. *Environ. Res. Lett.* **16**, 055025 (2021).
36. Wilkinson, G. M. et al. No evidence of widespread algal bloom intensification in hundreds of lakes. *Front. Ecol. Environ.* **20**, 16–21 (2021).
37. Carmichael, W. W. et al. Human fatalities from cyanobacteria: chemical and biological evidence for cyanotoxins. *Environ. Health Perspect.* **109**, 663–668 (2001).
38. Carmichael, W. W. The toxins of cyanobacteria. *Sci. Am.* **270**, 78–86 (1994).
39. Carmichael, W. W. & Boyer, G. L. Health impacts from cyanobacteria harmful algae blooms: implications for North American Great Lakes. *Harmful Algae* **54**, 194–212 (2016).
40. Codd, G. A., Morrison, L. F. & Metcalf, J. S. Cyanobacterial toxins: risk management for health protection. *Toxicol. Appl. Pharmacol.* **203**, 264–272 (2005).
41. Hilborn, E. D. & Beasley, V. R. One health and cyanobacteria in freshwater systems: animal illnesses and deaths are sentinel events for human health risks. *Toxins* **7**, 1374–1395 (2015).
42. Huisman, J. et al. Cyanobacterial blooms. *Nat. Rev. Microbiol.* **16**, 471–483 (2018).
43. Exley, G. et al. Floating photovoltaics could mitigate climate change impacts on water body temperature and stratification. *Sol. Energy* **219**, 24–33 (2021).
44. Ji, Q. et al. Effect of floating photovoltaic system on water temperature of deep reservoir and assessment of its potential benefits, a case on Xiangjiaba Reservoir with hydropower station. *Renewable Energy* **195**, 946–956 (2022).
45. Yang, P. et al. Impacts of floating photovoltaic system on temperature and water quality in a shallow tropical reservoir. *Limnology* **23**, 441–454 (2022).
46. Andini, S. et al. Analysis of biological, chemical, and physical parameters to evaluate the effect of floating solar PV in Mahoni Lake, Depok, Indonesia: mesocosm experiment study. *J. Ecol. Eng.* **23**, 201–207 (2022).
47. Château, P. A. et al. Mathematical modeling suggests high potential for the deployment of floating photovoltaic on fish ponds. *Sci. Total Environ.* **687**, 654–666 (2019).
48. Haas, J. et al. Floating photovoltaic plants: ecological impacts versus hydropower operation flexibility. *Energy Convers. Manage.* **206**, 112414 (2020).
49. Lee, N. et al. Hybrid floating solar photovoltaics-hydropower systems: benefits and global assessment of technical potential. *Renewable Energy* **162**, 1415–1427 (2020).
50. Stiubiener, U. et al. PV power generation on hydro dam's reservoirs in Brazil: a way to improve operational flexibility. *Renewable Energy* **150**, 765–776 (2020).
51. Dörenkämper, M. et al. The cooling effect of floating PV in two different climate zones: a comparison of field test data from the Netherlands and Singapore. *Solar Energy* **218**, 15–23 (2021).
52. Ziar, H. et al. Innovative floating bifacial photovoltaic solutions for inland water areas. *Prog. Photovoltaics* **29**, 725–743 (2021).
53. Gorjian, S. et al. Recent technical advancements, economics and environmental impacts of floating photovoltaic solar energy conversion systems. *J. Cleaner Prod.* **278**, 124285 (2021).
54. Armstrong, A. et al. Integrating environmental understanding into freshwater floatovoltaic deployment using an effects hierarchy and decision trees. *Environ. Res. Lett.* **15**, 114055 (2020).
55. Jane, S. F. et al. Widespread deoxygenation of temperate lakes. *Nature* **594**, 66–70 (2021).
56. North, R. P. et al. Long-term changes in hypoxia and soluble reactive phosphorus in the hypolimnion of a large temperate lake: consequences of a climate regime shift. *Glob. Change Biol.* **20**, 811–823 (2014).

57. Hupfer, M. & Lewandowski, J. Oxygen controls the phosphorus release from Lake Sediments—a long-lasting paradigm in limnology. *Int. Rev. Hydrobiol.* **93**, 415–432 (2008).
58. Bastviken, D. et al. Freshwater methane emissions offset the continental carbon sink. *Science* **331**, 50 (2011).
59. Vachon, D. et al. Influence of water column stratification and mixing patterns on the fate of methane produced in deep sediments of a small eutrophic lake. *Limnol. Oceanogr.* **64**, 2114–2128 (2019).
60. Cavaliere, E. & Baulch, H. M. Denitrification under lake ice. *Biogeochem. Lett.* **137**, 285–295 (2018).
61. Li, P. et al. Characteristic analysis of water quality variation and fish impact study of fish-lighting complementary photovoltaic power station. *Energies* **13**, 4822 (2020).
62. Al-Widyan, M. et al. Potential of floating photovoltaic technology and their effects on energy output, water quality and supply in Jordan. *Energies* **14**, 8417 (2021).
63. Bax, V. et al. Will it float? Exploring the social feasibility of floating solar energy infrastructure in the Netherlands. *Energy Res. Social Sci.* **89**, 102569 (2022).
64. Kumar, M. & Kumar, A. Experimental characterization of the performance of different photovoltaic technologies on water bodies. *Prog. Photovolt.* **28**, 25–48 (2020).
65. Sanchez, R. G. et al. Assessment of floating solar photovoltaics potential in existing hydropower reservoirs in Africa. *Renewable Energy* **169**, 687–699 (2021).
66. Birk, S. et al. Impacts of multiple stressors on freshwater biota across spatial scales and ecosystems. *Nat. Ecol. Evol.* **4**, 1060–1068 (2020).
67. Albert, J. S. et al. Scientists' warning to humanity on the freshwater biodiversity crisis. *Ambio* **50**, 85–94 (2021).
68. Exley, G. et al. Scientific and stakeholder evidence-based assessment: ecosystem response to floating solar photovoltaics and implications for sustainability. *Renewable Sustain. Energy Rev.* **152**, 111639 (2021).
69. Zhou, Y. L. et al. An advanced complementary scheme of floating photovoltaic and hydropower generation flourishing water–food–energy nexus synergies. *Appl. Energy* **275**, 115389 (2020).
70. Sulaeman, S. et al. Floating PV system as an alternative pathway to the Amazon dam underproduction. *Renewable Sustain. Energy Rev.* **135**, 110082 (2021).
71. Wang, S. et al. Future demand for electricity generation materials under different climate mitigation scenarios. *Joule* **7**, 309–332 (2023).
72. Chester, E. T. & Robson, B. J. Anthropogenic refuges for freshwater biodiversity: their ecological characteristics and management. *Biol. Conserv.* **166**, 64–75 (2013).
73. Messenger, M. L., Lehner, B., Grill, G., Nedeva, I. & Schmitt, O. Estimating the volume and age of water stored in global lakes using a geo-statistical approach. *Nat. Commun.* **7**, 13603 (2016).
74. Lehner, B. et al. High-resolution mapping of the world's reservoirs and dams for sustainable river-flow management. *Front. Ecol. Environ.* **9**, 494–502 (2011).
75. *Where Sun Meets Water: Floating Solar Handbook for Practitioners* (World Bank Group, ESMAP & SERIS, 2019).
76. Dzamesi, S. K. A. et al. Comparative performance evaluation of ground-mounted and floating solar PV systems. *Energy Sustain. Dev.* **80**, 101421 (2024).
77. Nisar, H. et al. Thermal and electrical performance of solar floating PV compared to on-ground PV system—an experimental investigation. *Sol. Energy* **241**, 231–247 (2022).
78. Rahaman, M. A. et al. Floating photovoltaic module temperature estimation: modeling and comparison. *Renewable Energy* **208**, 162–180 (2023).
79. Kim, K. Real options analysis for the investment of floating photovoltaic project in Saemangeum. *Korean J. Construct. Eng. Manage.* **22**, 90–97 (2021).
80. Pekel, J.-F., Cottam, A., Gorelick, N. & Belward, A. S. High-resolution mapping of global surface water and its long-term changes. *Nature* **540**, 418–422 (2016).
81. Ritchie, H., Roser, M. & Rosado, P. Energy. *Our World in Data* <https://ourworldindata.org/energy> (2022).
82. Schlömer, S. et al. in *Climate Change 2014: Mitigation of Climate Change* (eds Edenhofer, O. et al.) Annex III, 1335 (Cambridge Univ. Press, 2014); [https://www.ipcc.ch/site/assets/uploads/2018/02/ipcc\\_wg3\\_ar5\\_annex-iii.pdf](https://www.ipcc.ch/site/assets/uploads/2018/02/ipcc_wg3_ar5_annex-iii.pdf)
83. *Gridded Population of the World, Version 4 (GPWv4): Population Density, Revision 11* (SEDAC, 2019); <https://doi.org/10.7927/H49C6VHW>
84. Protected Planet: The World Database on Protected Areas (WDPA) (UNEP-WCMC & IUCN, 2023); [www.protectedplanet.net](http://www.protectedplanet.net)
85. Juffe-Bignoli, D. et al. Achieving Aichi biodiversity target 11 to improve the performance of protected areas and conserve freshwater biodiversity. *Aquat. Conserv. Mar. Freshwater Ecosyst.* **26**, 133–151 (2016).
86. Zhao, G. & Gao, H. Estimating reservoir evaporation losses for the United States: fusing remote sensing and modeling approaches. *Remote Sens. Environ.* **226**, 109–124 (2019).
87. Zhao, G. Floating photovoltaics power output for global lakes. *Figshare*. <https://doi.org/10.6084/m9.figshare.25764507.v1> (2024).

## Acknowledgements

This work was supported by the Third Xinjiang Scientific Expedition and Research (2021xjkk0800) and the Chinese Academy of Sciences Pioneer Initiative Talents Program. R.I.W. was supported by a UK Research and Innovation (UKRI) Natural Environment Research Council (NERC) Independent Research Fellowship (grant number NE/T011246/1). G.Z. was also supported by the Third Xinjiang Scientific Expedition Program (grant number 2021xjkk0803). We thank L. Feng (Southern University of Science and Technology, China) for making available the algal bloom occurrence data.

## Author contributions

R.I.W., A.A. and S.J.T. conceived the idea for this study. R.I.W., G.Z., A.A. and S.J.T. designed the methodology. G.Z. performed the large-scale model simulations. R.I.W. and G.Z. analysed the data with input from the other authors. R.I.W. led the writing of the manuscript, with input from A.A., S.J.T. and S.M.G.R. All authors contributed critically to the drafts and gave final approval for publication.

## Competing interests

The authors declare no competing interests.

## Additional information

**Supplementary information** The online version contains supplementary material available at <https://doi.org/10.1038/s44221-024-00251-4>.

**Correspondence and requests for materials** should be addressed to R. Iestyn Woolway.

**Peer review information** *Nature Water* thanks Rafael Almeida and Fi-John Chang for their contribution to the peer review of this work.

**Reprints and permissions information** is available at [www.nature.com/reprints](http://www.nature.com/reprints).

**Publisher's note** Springer Nature remains neutral with regard to jurisdictional claims in published maps and institutional affiliations.

**Open Access** This article is licensed under a Creative Commons Attribution 4.0 International License, which permits use, sharing, adaptation, distribution and reproduction in any medium or format, as long as you give appropriate credit to the original author(s) and the source, provide a link to the Creative Commons licence, and indicate if changes were made. The images or other third party material in this article are included in the article's Creative Commons licence, unless indicated otherwise in a credit line

to the material. If material is not included in the article's Creative Commons licence and your intended use is not permitted by statutory regulation or exceeds the permitted use, you will need to obtain permission directly from the copyright holder. To view a copy of this licence, visit <http://creativecommons.org/licenses/by/4.0/>.

© The Author(s) 2024